Ramesses and Radar:
A collaborative study of a tomb complex at South Asasif, Luxor, Egypt

Adam Booth[1,2], Tavi Murray[2], Kasia Szpakowska[3], Elena Pischikova[4]

1. Dept. of Earth Science & Engineering, Imperial College London, South Kensington Campus, London, SW7 2AZ, UK.
2. Glaciology Group, College of Science, Swansea University, Singleton Park, Swansea, SA2 8PP, UK.
3. College of Arts & Humanities: History and Classics, Swansea University, Singleton Park, Swansea, SA2 8PP, UK.
4. Director, South Asasif Conservation Project, Supreme Council of Antiquities, Egypt & American University in Cairo.

1. Abstract

Ground penetrating radar (GPR) datasets were acquired, in August 2011, in support of archaeological investigations at the South Asasif tomb complex (Luxor, Egypt). The goal of the GPR acquisitions was to image the extent of an ancient tomb beyond the current limits of its excavation, and specifically to image potential access points to the tomb's main chamber. Data were acquired using a Sensors and Software *pulseEKKO PRO* system, equipped with antennas of 200 MHz and 500 MHz centre frequencies. In addition to a common-offset grid (9 x 28 m) located above the target area, a number of calibration datasets were collected to assist interpretation, including vertical radar profiles (VRPs) and static reflectivity surveys over representative materials. The depth penetration of GPR energy at the site, ~ 1 m, was poorer than anticipated, attributable to the presence of organic-rich layers within the local desert sand. Nonetheless, the presence of archaeological structures was inferred from depressions in those layers, an interpretation that was reinforced following the partial excavation of a new chamber of the tomb. The specifics of the GEF loan were the 500 MHz GPR antennas, obtained via an emergency grant after the system we planned to deploy developed a fault.

2. Background

The tomb of the high-priest *Karakhamun* (Theban Tomb (TT) 223; 25°43'45.05" N, 32°36'23.45" E) is the largest and highest-status of several burial sites at the South Asasif tomb complex (Figure 1). Dating from the 25th and 26th Dynasties of ancient Egypt (760-525 BC), the South Asasif tombs were described as 'beautiful' by 18th century travellers but were rediscovered in 2006 in a dilapidated state. They have since undergone extensive conservation and restoration, and TT223 has been partly excavated. Immediately adjacent to TT223 are the tombs of *Anchefendhout* (TT C14) and *Irtieru* (TT390), and that of *Karabasken* (TT391) is further west. Each of these tombs is in better condition, but smaller and less-ornate than that of *Karakhamun* (Pischikova, 2008, 2009).

Currently, excavations of TT223 have revealed two 'pillared halls' (Figures 1 and 2a) and a sunken burial chamber, but the entrance and vestibule of the tomb are yet to be uncovered. Tombs with similarly high-status, including that of *Pabasa* (TT279; Figure 2b), typically feature a stone staircase that descends from the surface to an entrance hall at the subsurface level of the pillared halls. GPR methods were therefore explored for any similar structures extending east from the current limit of the TT223 excavation, and to recommend thereafter a site for future excavation.

3. Tomb Construction and Detection Potential

The superstructure of the South Asasif tombs is cut into natural limestone (see sand/limestone contact in Figure 1*ii*). TT223 is overlaid by ~ 2 m of desert sand, and its limestone roof is around 1 m thick. Although the unexcavated part of the tomb is expected to be filled with desert sand, air-gaps often remain between the underside of the roof and the sediment fill. Given the desert setting, subsurface water content is expected to be low therefore signal penetration was expected to be good, hence we anticipated that the tomb roof should be detectable with 200 MHz antennas, if not 500 MHz.

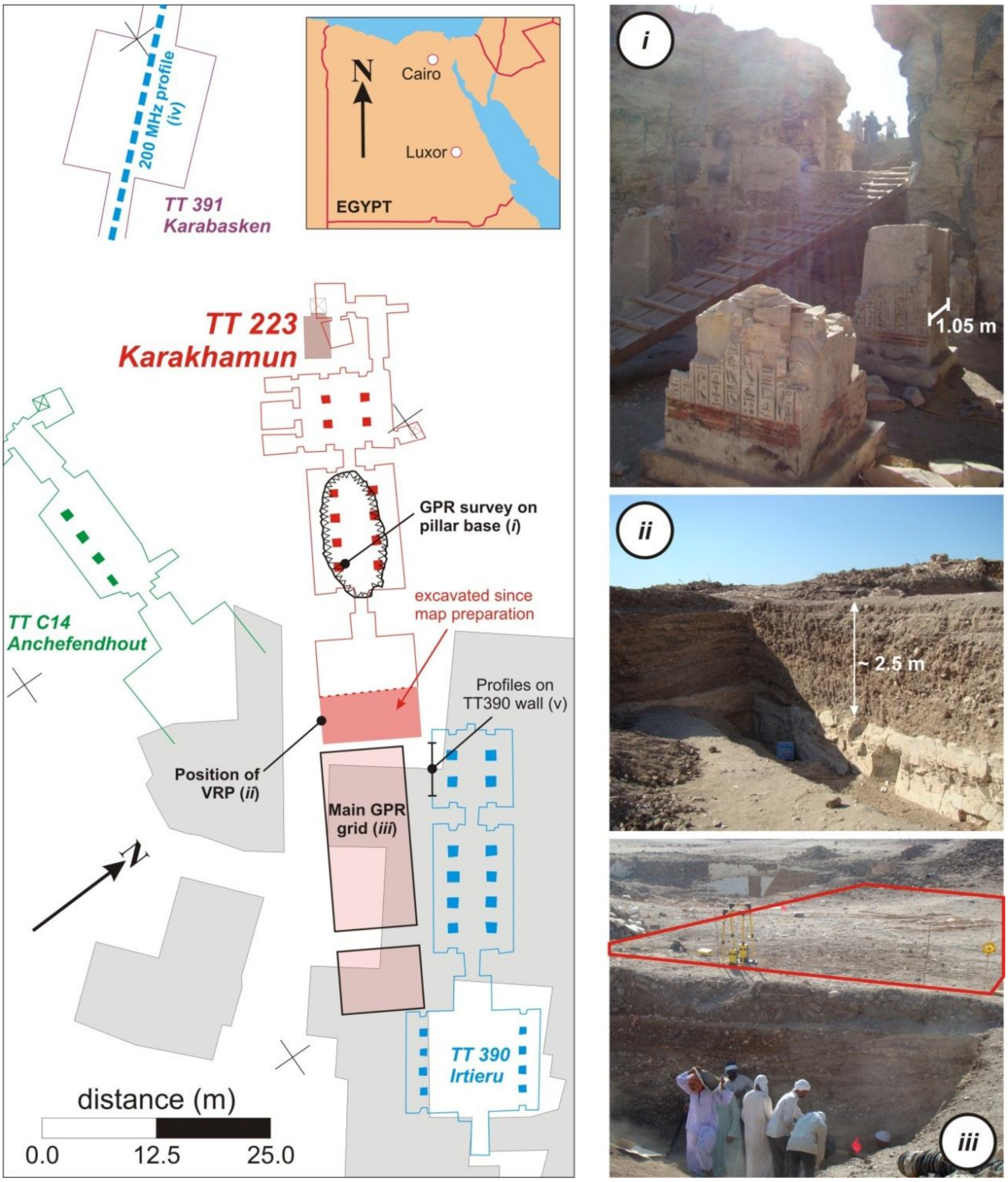

Figure 1. Location map, with four of the South Asasif tombs (digitised from Eigner, 1980), including that of *Karakhamun* (TT223, red outline); location in Egypt inset. Grey areas show areas previous occupied by huts. All tombs are subsurface, except for excavated regions of TT223. Labels (*i*-*v*) show the locations of GPR surveys described in this report. ***i*)** 500 MHz calibration survey on of pillar (corresponding photo looks east, from inside TT223; the pillar surveyed is 1.05 m thick). ***ii*)** 500 MHz VRP survey in tomb overburden (corresponding photo looks south-east from inside area of recent excavation); note the sharp contact between the limestone superstructure of the tomb and its sediment overburden. ***iii*)** Main GPR grid, immediately east of the current edge of TT223 excavation (photo looks east, from the southern side of the TT223 excavation). ***iv*)** 200 MHz test survey over TT391. ***v*)** 500 MHz profiles on the internal wall of TT390.

However, this apparently straightforward task was complicated by the fact that, until recently, South Asasif was also occupied by a village (extent in Figure 1). Not only were buildings constructed close to the target area, vacant areas and exposed tombs themselves were occupied by farm animals. Not only has this damaged the archaeological remains, it also complicates the geophysical survey, firstly by limiting access across the site and secondly by degrading the GPR response; several areas of the site are covered by building rubble, and centuries of farming has left 'organic-rich layers' within the natural desert sand, which are attenuative to radar energy (e.g., Weaver, 2006).

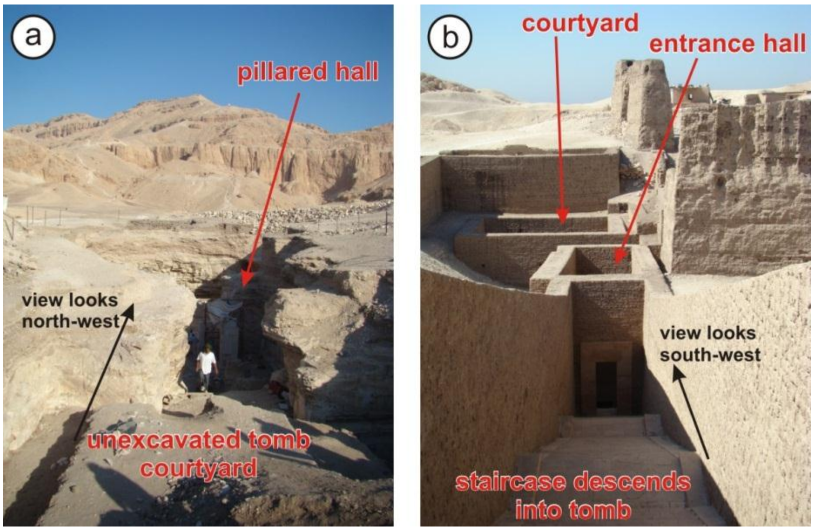

Figure 2. Photos from the tombs of a) *Karakhamun* (TT223) and b) *Pabasa* (TT279), analogous to TT223. The relative viewing angle is the same for both photos, i.e., looking from the exterior of each tomb into its interior. TT279 shares many features with TT223, but the descending staircase into the latter is not yet identified and excavated.

Given these concerns about signal attenuation and depth penetration, test surveys were performed prior to the main survey of TT223. To test propagation through the local limestone, 500 MHz antennas were held against a standing section of a square, limestone pillar (1.05 m thick; Figure 1*i*) within the main hall of TT223, and a number of traces were recorded. Primary reflections *and* the first-multiple from the opposite face of the pillar were visible(Figure 3a), suggesting that 500 MHz GPR energy can propagate over 4 m (2 m two-way distance) through local limestone and still be detectable (the travel-time of these arrivals suggests that the GPR velocity through limestone is 0.13 m/ns). By comparison, a vertical radar profile (VRP; Buursink *et al.*, 2002) on an exposed section of organic-rich layers (Figures 1*ii* and 3b) suggested that the penetration of 500 MHz energy would be no greater than in a typical temperate setting, allowing a maximum depth of ~1 m to be sampled; the corresponding velocity was measured at 0.11 m/ns.

Finally, a 200 MHz common-offset (CO) profile was performed over the known superstructure of TT391 (Figure 1, label *iv*) to investigate depth penetration with the lower-frequency system; no reflections from the tomb could be detected. Although TT391 is located beneath a thicker sediment cover, the potential to image the superstructure of TT223, with either 500 or 200 MHz antennas, was therefore deemed to be low.

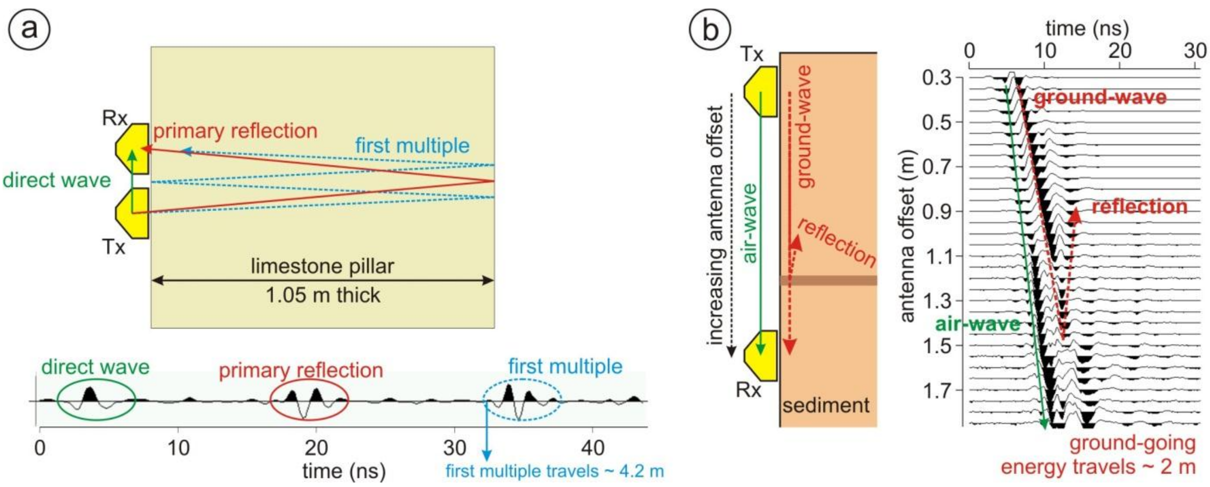

Figure 3. Calibration datasets and schematic representations of their acquisition. a) Static reflectivity analysis, with transmitting (Tx) and receiving (Rx) GPR antennas placed on the wall of a limestone pillar (Figure 1*i*). The first multiple raypath (blue) travels four times the thickness of the pillar, hence energy is still detectable after propagating for over 4 m. GPR trace is scaled using automatic gain control. B) Vertical radar profile (VRP), in which Tx and Rx are vertically offset while held against the an exposed sediment wall (Figure 1*ii*). Ground-going energy (red) is not detectable after propagating for ~ 2 m.

However, the GPR profiles did contain strong reflections from the organic-rich layers within the sediment cover (see Figure 4, next section), and the presence of archaeological structures may therefore be inferred from changes in their geometry.

4. Main GPR Survey and Preliminary Results

A pseudo-3D grid of 500 MHz CO profiles was acquired east of the limit of the TT223 excavation on completely level ground (Figure 1*iii*). The grid has dimensions of 9 x 28 m, with in-line and cross-line sampling intervals of 0.05 m and 0.25 m, respectively (possibly allowing interpolation to full-3D sampling criteria; Booth *et al.*, 2008). All profiles were orientated perpendicular to the long-axis of TT223, and acquisitions were triggered using a calibrated odometer wheel. A standard processing sequence was applied to all data, using Sandmeier *ReflexW*©, including dewow (5 ns time window) and bandpass (corner frequencies of 120-200-500-1100 MHz) filters, time-zero static corrections and Kirchhoff migration (using a velocity and migration aperture of 0.11 m/ns and 1 m, respectively). Representative profiles and depth-slices from this grid are shown in Figure 4.

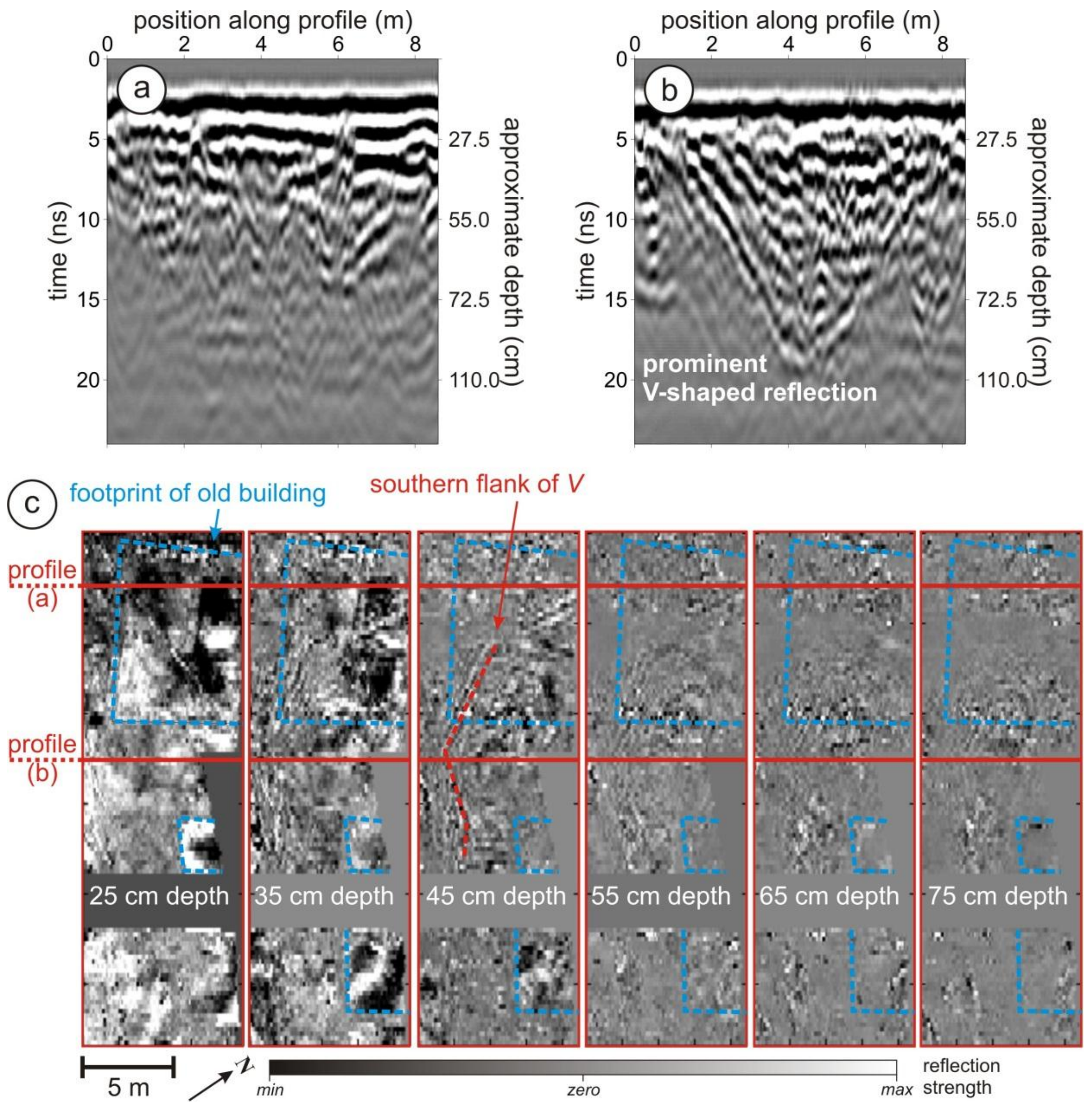

Figure 4. 500 MHz GPR data acquired in the main grid, east of the TT223 excavation. Certain CO profiles show little subsurface reflectivity (e.g., a) whereas others feature a prominent, spatially continuous *V-shaped* reflection (e.g., b) interpreted as a horizon within the sediment overlying the tomb. Depth-slices through the grid (c) show the southern flank of the *V* moving towards the north of the grid with increasing depth (red-dashed line marks its position in 45 cm depth slice; the blue dashed lines mark the footprint of earlier, now-demolished buildings). For reference, the position of the profiles in (a) and (b) is marked in each slice. The gap in data coverage is due to the presence of concrete rubble at surface.

In Figure 4b there is a prominent '*V-shaped*' reflection that is absent in (a). This reflection becomes more prominent, and deeper, with increasing distance from the tomb, and is best-defined some 18 m from the western edge of the grid. The southern flank of the reflector is particularly clear in time-slices (Figure 4c), and progressively moves north across the grid with increasing depth. To highlight the geometry of the *V-shaped* reflector, Figure 5 shows a colour-contoured map of its depth as measured in the GPR grid (assuming a velocity of 0.11 m/ns). Clearly, the reflectors define a closed, bowl-shaped anomaly, the trend of which is closely aligned with the long-axis of TT223 (black dashed line).

Reflectivity may have been partly masked beneath the site of previous construction (grey, Figure 5) hence it was also investigated from within the accessible main chamber of the *Irtieru* tomb (TT390). If the superstructure of TT223 does continue east, with a similar width to that already observed in excavation, there is a strong likelihood that it will pass close to the edge of TT390. We previously established that 500 MHz GPR energy could propagate over 4 m through the local limestone, hence if a wall of TT223 is within 2 m of TT390 (hashed area in Figure 5), it may be detectable as a vertically-orientated reflector. Some weak reflectivity was observed in these profiles, potentially originating from the continuation of TT223, but this could not be unambiguously distinguished from other potential noise sources within the *Irtieru* tomb. The use of 200 MHz antennas could have allowed further penetration into the tomb wall but, since these are unshielded, they are unsuitable for use within the enclosed space of the tomb.

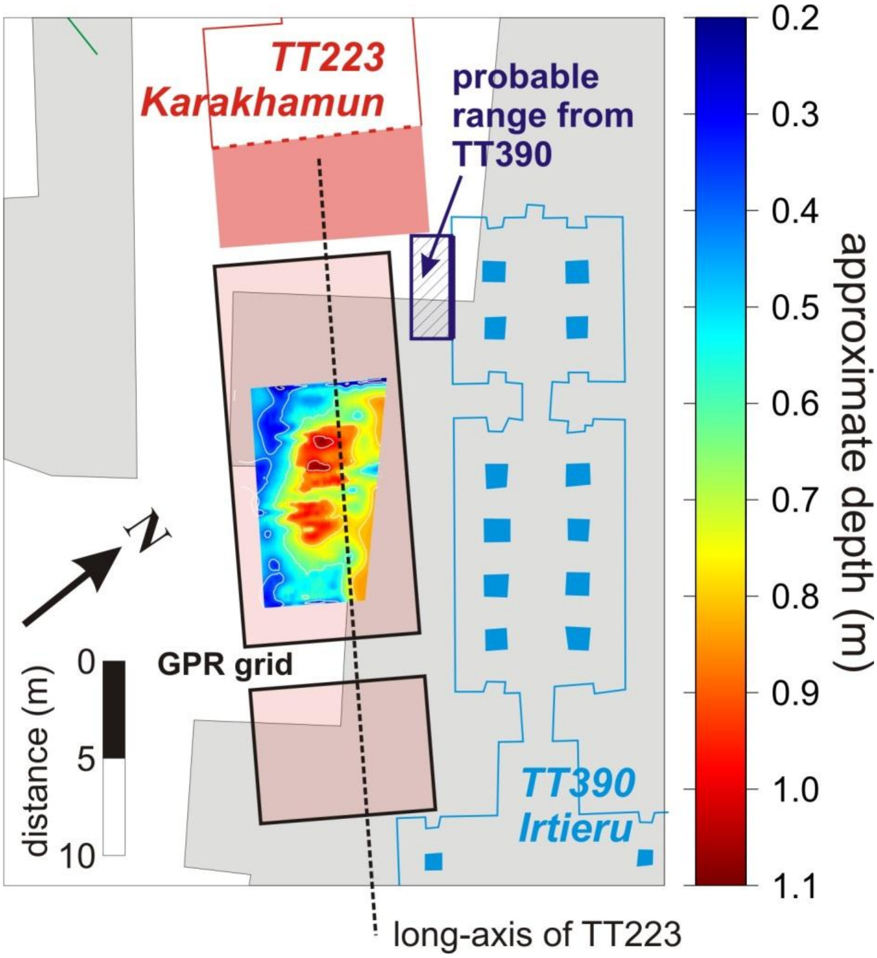

Figure 5. Colour-contoured map of the depth of the *V-shaped* reflections, east of TT223. The reflectors define a closed, bowl-shaped anomaly the trends close to the long-axis of the tomb (black dashed line). Some reflectivity was detected in CO profiles acquired on the internal wall of the *Irtieru* tomb (TT390), but these do not unambiguously confirm whether or not the superstructure of TT223 passes within ~2 m (hashed area) of TT390.

5. Interpretation and Outlook

If the assumption is correct that deflected organic reflectors are associated with underlying archaeology, the *V-shaped* reflector could diagnose a continuation of TT223. Figure 6 shows schematic scenarios describing how the deflected horizons could be associated with tomb structure, potentially indicative of a collapsed or open-roofed structure. Both of these scenarios are possible at TT223: collapses are known (indeed, in part of TT223 itself) as the local limestone is somewhat fractured, and the staircase into the analogous *Pabasa* tomb has no roof. If an organic layer is initially deposited over an intact or roofed structure, we assume that it will be horizontal (Figure 6a). If there is a subsequent collapse, the layers should be deflected downwards in response (Figure 6b), and will be similarly deflected if underlying sediment progressively settles into an open structure such as a rock-cut staircase (Figure 6c), thereby forming the V-*shaped* reflector. The absence of a *V* would clearly not imply the absence of archaeology (it could simply be that no layers were deposited at that location), but an archaeological explanation is possible where the *V* is observed whichever scenario is correct.

These hypotheses were part-validated at the end of the GPR campaign. Throughout the survey, excavations had been continuing in the chamber of TT223 and revealed the lintel of a doorway in the eastern tomb wall. By the final day of surveying, the excavation had progressed sufficiently to allow access to a new part of the superstructure: a small chamber, some 2.5 m wide and 5 m long (north-south and east-west dimensions, respectively), with evidence of a doorway at its far end and – critically – a developing roof collapse (Figure 7). Importantly, this extension of the superstructure does not pass sufficiently close to the internal wall of TT390 to be detectable from within. The excavation and GPR records therefore indicate that there is almost certainly an eastwards continuation of the *Karakhamun* tomb, although it may be in a poor state of preservation. New excavations were therefore recommended at the centre of the anomaly in Figure 5 (red hashed area, Figure 7).

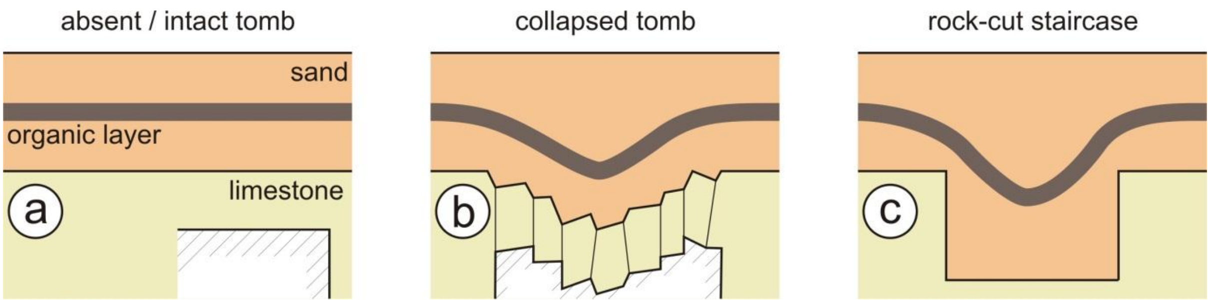

Figure 6. Schematic representations of the formation of the V-shaped organic reflectors observed in the GPR data. a) If organic layers are deposited over an absent or intact tomb, which does not subsequently collapse, no *V* will be observed. b) If the tomb subsequently collapses, the organic layers may be deflected downwards and a *V* will be observed. c) A *V* may develop if sediment is deposited over, and settles into, the hollow represented by a rock-cut staircase.

6. Instrument Deployment Details

There were no operational issues in using the GPR antennas loaned from the GEF (via an emergency application following a fault on the equipment we expected to use), and they were in perfect working order throughout the duration of the survey. The equipment arrived at Swansea University on time, and was returned to the GEF at the end of the loan period.

The biggest challenge encountered was clearing the GPR system through Egyptian customs (despite governmental permission to perform the survey) and the resulting delay effectively halved the time spent in the field. We would recommend that survey groups working in the area make scheduling allowances for equivalent delays, and that the signatures of all relevant authorities are obtained prior to entering the country.

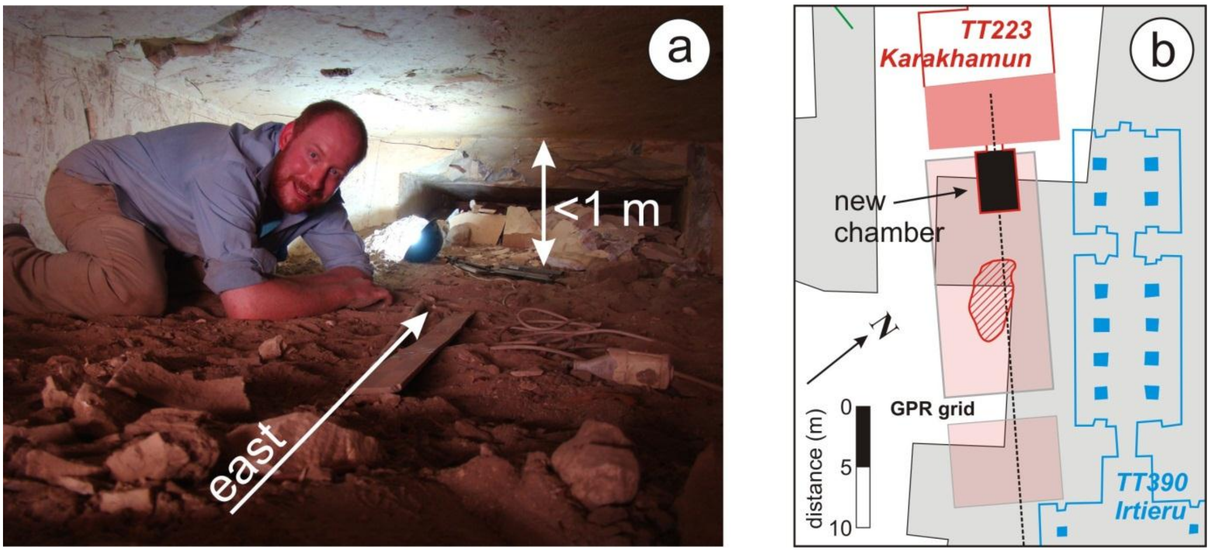

Figure 7. a) Photograph inside newly excavated chamber of TT223 (no excavation has taken place inside the chamber – the air-gap, less than 1 m thick, was already present in the subsurface). The chamber extends parallel to the long axis of TT223. b) New chamber (black box) added to the map of TT223. Based on the archaeological and geophysical evidence, future excavations were recommended at the centre of the *V-shaped* reflectors (marked by the red hashed area).

7. Relevant Publications and Presentations

Pischikova E (2011); *Dancers, Donkeys and Dirt: New discoveries from the time of the Black Pharaohs from South Asasif, Egypt*; Research Institute for Arts and Humanities Public Lecture Series, Swansea University.

Li N (2012); Trace interpolation for anti-aliasing and 2-D migration image improvement; Unpublished MSc Thesis, Imperial College London.

8. References

- Booth AD, Linford NT, Clark RA and Murray T (2008); Three-dimensional, multi-offset ground penetrating radar imaging of archaeological targets; Archaeological Prospection, 15(2), 93-112.
- Buursink ML, Lane JW, Clement WP and Knoll MD (2002); Use of vertical radar profiling to estimate porosity at two New England sites and comparison with neutron porosity log; Symposium on the Application of Geophysics to Engineering and Environmental Problems, Las Vegas, Nevada.
- Eigner D (1980); *Südliches Asasif*; 1:500 scale map of South Asasif Tomb Complex.
- Pischikova E (2008); Tomb of Karakhamun (TT 223) in the South Asasif and a "Lost" Capital; Journal of the American Research Center in Egypt, 45.
- Pischikova E (2009); The early Kushite Tombs of South Asasif; British Museum Studies in Ancient Egypt and Sudan, 12, 11-30.
- Weaver W (2006); GPR mapping in clay: success from South Carolina, UAS; Archaeological Prospection, 13, 147-150.

9. Acknowledgments

This project was funded by the Swansea University 'Bridging the Gaps' initiative. The Egyptian Supreme Council for Antiquities granted access to the South Asasif tombs. Ken Griffin and Meg Gundlach provided invaluable logistical support.